RESEARCH ARTICLE

VOL. 45 | NO. 3 |**SEPTEMBER - DECEMBER 2024** | PP 6-19

Revista Mexicana de Ingeniería Biomédica

dx.doi.org/10.17488/RMIB.45.3.1

E-LOCATION ID: 1428

A Real-Valued Kalman Estimation Method for Harmonic Signal Analysis in Biomedical Applications

Análisis de Señales Biomédicas por Medio del Método de Estimación Armónica de Kalman con un Modelo de Valores Reales

Johnny Rodríguez-Maldonado[1], *Miguel Angel Platas-Garza*[1], *Ernesto Zambrano-Serrano*[1]

[1]Universidad Autónoma de Nuevo León, Nuevo León - México

ABSTRACT

This work presents a methodology for obtaining the harmonic estimation of biomedical signals such as electrocardiogram, cardiorespiratory and blood pressure signals. The proposed methodology is achieved using polynomial approximation and the Kalman filter. As advantage, the technique includes instant estimations of signal harmonics and its derivatives using a real-valued model. Furthermore, a comparison of the results is conducted with the Savitzky-Gola, nonlinear tracking differentiator methods, extended state observer and digital differentiator base on Taylor series. The results suggest that the proposed method has the potential to enhance the quality of signal measurements, especially in the presence of noise.

KEYWORDS: biomedical signal analysis, harmonics estimates in ECG, derivative estimation in biomedical signals

RESUMEN

Este trabajo presenta una metodología para obtener la estimación armónica de señales biomédicas como señales de electrocardiograma, cardiorrespiratorias y de presión arterial. La metodología propuesta utiliza la aproximación polinomial y el filtro de Kalman. Como ventaja, la técnica incluye estimaciones instantáneas de las armónicas de la señal y sus derivadas utilizando un modelo con parámetros en los reales. Además, se realiza una comparación de los resultados con los métodos de Savitzky-Golay, el diferenciador de seguimiento no lineal, observador de estados extendido y diferenciador digital basado en series de Taylor. Los resultados sugieren que el método propuesto tiene el potencial de mejorar la calidad de las mediciones de señales, especialmente en presencia de ruido.

PALABRAS CLAVE: **análisis de señales biomédicas, estimación armónica en señales biomédicas, estimación de derivadas en señales biomédicas**

Corresponding author

TO: Johnny Rodríguez-Maldonado

INSTITUTION: Universidad Autónoma de Nuevo León, Nuevo León - México

ADDRESS: Pedro de Alba S/N Entre Av. Alfonso Reyes y Av. Fidel Velázquez, Ciudad Universitaria. San Nicolás de los Garza, Nuevo León, México.

EMAIL: johnny.rodriguezml@uanl.edu.mx

Received:

23 April 2024

Accepted:

9 August 2024

INTRODUCTION

Signal analysis is essential in many engineering fields, including power systems, vibration analysis, voice recognition, radar applications, biomedical engineering, and digital communications. Because it allows obtaining relevant features regarding system information. The human body has different systems, such as the cardiovascular, nervous, and respiratory system, among others[1]. From these systems, signals can be obtained that provide relevant information. These signals are processed for analysis[2][3], which leads to their quantization, causing quantization error. These signals can not only be affected by quantization error but also by other errors caused by measurement instrument components or incorrect usage. One solution to this issue is the implementation of a methodology that considers noise filtering and achieves instantaneous estimates without the need for a sample window for estimation.

The measurement of biomedical signals is a cornerstone of modern healthcare, providing critical insights into physiological processes and aiding in the diagnosis and treatment of various medical conditions. Common examples of biomedical signals are electrocardiograms (ECG), electroencephalograms (EEG), and blood pressure measurements. These signals are crucial for monitoring patient health, conducting medical research, and developing new medical technologies. The precision and capabilities of biomedical signal measurement depend on sensors and signal processing techniques. Digital Signal Processing (DSP) techniques enable the extraction of meaningful information from noisy signals, improving diagnostic accuracy[4]. Therefore, the rates of change in biomedical signals are part of their analysis.

Below are some methodologies that can be implemented in signal estimation, which can also estimate the rate of change in the signal. The Savitzky-Golay (Sgolay) method includes the use of data windows[5][6], introducing a delay in its estimates. In[7][8], the discrete wavelet transform is implemented to cancel disturbances in ECG caused by devices or movements. However, even when the sample window size can be narrow depending on the signal resolution to be estimated, a sample window is still necessary for information estimation. On the other hand, the Nonlinear Tracking Differentiator (NTD) method[9][10] requires an adjustment parameter, which consequently implies a drawback since this parameter needs to be calibrated with respect to the signal to be estimated, leading to potentially suboptimal or highly suboptimal estimates. In response to these limitations and based on the results obtained from the methodology used in[11][12] for phasor estimation, it was proposed to employ a methodology that enables instant estimations. This methodology is grounded in the implementation of a signal model that includes its respective derivatives, all within a state transition matrix. With a zeroth-order model (approximating the signal with a zeroth-order Taylor polynomial), estimations of the electrocardiogram are obtained. By increasing the order of the Taylor polynomial, the model is modified, allowing for the estimation of signal derivatives, achieving a better response in estimation for signals corrupted by noise. This methodology surpasses the limitations of other strategies in the sense that there is no need for a sample window to perform estimations and enables a more accurate signal approximation by reducing noise. Consequently, the proposed method focuses on obtaining a more precise and comprehensive estimation in relation to the characteristics of biomedical signals. It successfully provides good estimates for signals such as electrocardiograms, cardiorespiratory signals, and blood pressure. Another method that can be implemented in the analysis of biomedical signals is the Extended State Observer (ESO), proposed for the cascade of integrator systems without measurement noise[13][14].

In the monitoring of ECG, it is common to use modulation techniques for transmission and reception. Some techniques have been developed; for example, in[15], a real-time algorithm for ECG-Derived Respiration is presented. In[16], an adaptive algorithm using different modulation schemes is introduced. In[17], a method for ECG monitoring is proposed that utilizes a transmitter-receiver system with modulation frequencies to send and receive ECG information.

Achieving a better representation of an ECG signal is another objective. For instance, in [18], a method to obtain a better representation of blood flow signals was proposed. In[19], a novel ECG enhancement algorithm based on sparse derivatives is introduced. In[20], the ECG is viewed as a quasi-periodic process and employs the unbiased finite impulse response (UFIR) smoother on optimal horizons, applied to a harmonic ECG model with good results. In[21], a new tracking differentiator is proposed, which can synchronously filter noise and estimate the derivative of the input signal. The proposed method, based on the analysis of the rate of changes in some biomedical signals such as ECG and blood pressure, involves the development of a model using a passband signal and its derivatives. By approximating the signal and its derivatives with Taylor polynomials, it is possible to develop a state transition to implement in the Kalman filter. Since the proposed method uses Taylor polynomials, the methodology is compared with a Digital Differentiator based on Taylor Series (DDTS)[21].

The aim of this work is to present a method to estimate the derivative signal of an ECG. With the derivative, it is possible to detect high frequencies in the ECG, which are common in coronary heart disease and useful for electrocardiographic diagnosis. In[22], the derivative of an ECG is obtained using an electronic circuit and operational amplifier. However, in this document, the derivative is obtained mathematically, and the algorithm can be implemented in any microcontroller, DSP, FPGA, or PC. Additionally, the numerical results can be obtained in real time, and the method only needs one sample to achieve the estimate of both the signal and its derivative.

MATERIALS AND METHODS

Commonly, biological systems produce quasi-periodical signals. These signals are almost periodical signals, but with fluctuations between periods. Next, the model shown in[12][23] for a quasiperiodic signal oscillation is presented.

We start using a periodical signal $s_p(t)$, a fundamental approach involves to represent a periodic signal by its Fourier representation in Equation 1:

$$s_p(t) = \sum_{h=-H}^{H} c_h e^{jh\omega_1 t}, \tag{1}$$

where ω_1 represents the fundamental frequency in radians per second, H is the number of harmonics considered, and c_h represents the Fourier coefficient related to the h-th harmonic.

If (1) is relaxed to allow slow variations (compared with ω_1) in c_h in both amplitude and phase, then the expression

$$c_h(t) = a_h(t)e^{j\varphi_h(t)}, \tag{2}$$

can be used to model the fluctuation through the behavior of each coefficient, where $a_h(t)$ and $\varphi_h(t)$ now represent the amplitude and phase variation for each harmonic. Under the assumption (Equation 2), the quasi-periodic version of $s_p(t)$ is given by

$$s(t) = \sum_{h=-H}^{H} c_h(t) e^{jh\omega_1 t}, \tag{3}$$

where for a real-valued signal (Equation 3), the components should meet $\overline{c_h(t)} = c_{-h}(t)$ for $h \neq 0$, with $\overline{c_h(t)}$ representing the complex conjugate of $c_h(t)$. This relaxed model offers more flexibility as it allows the description of the time-varying dynamic evolution of each harmonic. The Taylor series at t_0 can be used to represent each passband signal (Equation 4) by:

$$c_h(t) = \sum_{k=0}^{K} c_h^{(k)}(t_0) \frac{(t-t_0)^k}{k!} \varepsilon_h^{(k+1)}(t), \tag{4}$$

with $c_h^{(k)}(t_0) = \frac{d^k c_h t_0}{dt^k}\Big|_{t=t_0}$ representing the k-th derivative of the h-th harmonic at $t = t_0$, and $\varepsilon_h^{(k+1)}(t)$ representing the residue due to higher-order terms.

Using (Equation 4) in (Equation 3), the following ex-pressing is obtained for the quasi-periodical signal (Equation 5):

$$s(t) = \sum_{h=-H}^{H} r_h(t) + \mathrm{E}(t), \tag{5}$$

where

$$r_h(t) = \sum_{k=0}^{K} \frac{c_h^{(k)}(t_0)}{k!} (t-t_0)^k e^{jh\omega_1 t}, \tag{6}$$

represents the h-th rotated phasor, and $\mathrm{E}(t)$ represents the summation over of the residues $\mathrm{E}(t) = \sum_{h=-H}^{H} \varepsilon_h^{(k+1)}(t)$.

The relation (Equation 6) can be used to construct a transition function for the rotated phasor from time t_0 to time t. We construct it by analyzing (Equation 6) per each value of h. We separate two cases, $h = 0$ and $h \neq 0$.

First, for $h = 0$, the DC component $r_0 = c_0$ at instant t can be related to t_0 by performing the derivation of (Equation 6) $(K-1)$ times (Equation 7):

$$\boldsymbol{r}_0(t) = \boldsymbol{\Psi}(t-t_0) r_0(t_0), \tag{7}$$

where the i-th element o the vector $\boldsymbol{r}_0(t) \in \mathbb{R}^{(K+1)}$ is given by the i-th **derivative** of the DC component $c_0^{(i)}(t)$ for $i = 1, \ldots, n$; and the i-th element of the j-th column of the matrix $\boldsymbol{\Psi}(t-t_0) \in \mathbb{R}^{(K+1)\times(K+1)}$ is given by (Equation 8):

$$\psi_{i,j}(t) = \begin{cases} 0, & i > j, \\ \dfrac{(t-t_0)^{(j-i)}}{(j-i)!}, & i \leq j. \end{cases} \tag{8}$$

In a similar manner, for $h \neq 0$ the k-th harmonic component h at instant t can be related to t_0 by performing the derivation of (6) $(K-1)$ times, where now, due to the complex exponential function, we have (Equation 9):

$$r_h(t) = \boldsymbol{M}(h\omega)\boldsymbol{\Psi}(t - t_0)\boldsymbol{M}^{-1}(h\omega)e^{jh\omega_1 t}\boldsymbol{r}_h(t_0). \tag{9}$$

In this context, the i-th element of $\boldsymbol{r}_h(t) \in \mathbb{C}^{(K+1)}$, in (9) represents the i-th derivative of $r_h^{(i)}(t)$ and $\boldsymbol{M}(h\omega) \in \mathbb{C}^{(K+1)\times(K+1)}$ is a lower triangular complex matrix with elements given by (Equation 10):

$$m_{r,c} = \begin{cases} 0, & r < c, \\ 1, & r = c, \\ \dfrac{(r-1)!}{(c-1)!(r-c)!}(jh\omega)^{(r-c)}, & r > c. \end{cases} \tag{10}$$

A discrete representation of (Equation 10) can be obtained sampling $s(t)$ with a uniform sampling time T, and using $t_0 = nT$ and $t = (n + 1)T$, it is possible to use the relations in (Equation 9) to relate the rotated phasor from sample to sample. From (Equation 9), with $t_0 = nT$ and $t = (n + 1)T$ we have (Equation 11):

$$\boldsymbol{r}_h(n + 1) = \boldsymbol{\Phi}_h(n + 1, n)\boldsymbol{r}_h(n), \qquad h = -H, \ldots, H \tag{11}$$

where $\boldsymbol{\Phi}_h(n + 1, n) = \boldsymbol{M}(h\theta)\boldsymbol{\Psi}(T)\boldsymbol{M}^{-1}(h\theta)e^{jnh\theta_1}$ works as a transition matrix from time nT to $(n + 1)T$, and θ_1 represents the discrete fundamental frequency in radians.

Using (Equation 11) to represent each component in (Equation 5), a model for the signal $s(n)$ can be constructed as follows (Equation 12):

$$\begin{aligned} \boldsymbol{x}(n + 1) &= \boldsymbol{A}\boldsymbol{x}(n), \\ s(n) &= \boldsymbol{C}\boldsymbol{x}(n) + \mathrm{E}(n), \end{aligned} \tag{12}$$

where $\boldsymbol{x} \in \mathbb{C}^{(2H+1)(K+1)}$ represents a vector formed from the union of the $2H + 1$ vectors $\boldsymbol{r}_h$, the components are ordered as follows $\boldsymbol{x} = [\boldsymbol{r}_0 \;\; \boldsymbol{r}_1 \;\; \boldsymbol{r}_{-1} \;\; \boldsymbol{r}_2 \;\; \boldsymbol{r}_{-2} \;\; \ldots \;\; \boldsymbol{r}_H \;\; \boldsymbol{r}_{-H}]'$; thereby following (11) the matrix $\boldsymbol{A} \in \mathbb{C}^{(2H+1)(K+1)\times(2H+1)(K+1)}$ is a block diagonal matrix given by (Equation 13):

$$\boldsymbol{A} = \begin{bmatrix} \boldsymbol{\Phi}_0 & \mathbf{0} & \mathbf{0} & \ldots & \mathbf{0} & \mathbf{0} \\ \mathbf{0} & \boldsymbol{\Phi}_1 & \mathbf{0} & \ldots & \mathbf{0} & \mathbf{0} \\ \mathbf{0} & \mathbf{0} & \boldsymbol{\Phi}_{-1} & \ldots & \mathbf{0} & \mathbf{0} \\ \vdots & \vdots & \vdots & \ddots & \vdots & \vdots \\ \mathbf{0} & \mathbf{0} & \mathbf{0} & \ldots & \boldsymbol{\Phi}_H & \mathbf{0} \\ \mathbf{0} & \mathbf{0} & \mathbf{0} & \ldots & \mathbf{0} & \boldsymbol{\Phi}_{-H} \end{bmatrix}, \tag{13}$$

and $\boldsymbol{C} \in \mathbb{R}^{(2H+1)(K+1)}$ represents the synthesis of the signal from its harmonic components, according to (Equation 5) $\boldsymbol{C}$ is given by the union of $(2H + 1)$ blocks $\xi \in \mathbb{R}^{K+1}$, where $\xi = [1 \quad 0 \quad \ldots \quad 0]$.

Only for $h = 0$ the corresponding elements in $\boldsymbol{A}$ and $\boldsymbol{x}$ are real-valued. However, a real-valued version of (Equation 12) can be obtained using $\overline{c_h(t)} = c_{-h}(t)$ for $h \neq 0$. We use the following linear transformation $\tilde{\boldsymbol{x}} = \boldsymbol{P}\boldsymbol{x}$ where $\tilde{\boldsymbol{x}} \in \mathbb{R}^{(2H+1)(K+1)}$ (Equation 14):

$$\begin{bmatrix} \boldsymbol{r}_0 \\ \mathrm{Re}(\boldsymbol{r}_1) \\ j\mathrm{Im}(\boldsymbol{r}_1) \\ \vdots \\ \mathrm{Re}(\boldsymbol{r}_h) \\ j\mathrm{Im}(\boldsymbol{r}_h) \end{bmatrix} = \begin{bmatrix} \mathbf{I} & \mathbf{0} & \mathbf{0} & \dots & \mathbf{0} & \mathbf{0} \\ \mathbf{0} & \frac{1}{2}\mathbf{I} & \frac{1}{2}\mathbf{I} & \dots & \mathbf{0} & \mathbf{0} \\ \mathbf{0} & -j\frac{1}{2}\mathbf{I} & j\frac{1}{2}\mathbf{I} & \dots & \mathbf{0} & \mathbf{0} \\ \vdots & \vdots & \vdots & \ddots & \vdots & \vdots \\ \mathbf{0} & \mathbf{0} & \mathbf{0} & \dots & \frac{1}{2}\mathbf{I} & \frac{1}{2}\mathbf{I} \\ \mathbf{0} & \mathbf{0} & \mathbf{0} & \dots & -j\frac{1}{2}\mathbf{I} & j\frac{1}{2}\mathbf{I} \end{bmatrix} \begin{bmatrix} \boldsymbol{r}_0 \\ \boldsymbol{r}_1 \\ \boldsymbol{r}_{-1} \\ \vdots \\ \boldsymbol{r}_H \\ \boldsymbol{r}_{-H} \end{bmatrix}, \tag{14}$$

Using the lineal transformation (Equation 14), a real-valued representation of (Equation 12) is (Equation 15):

$$\begin{aligned} \tilde{\boldsymbol{x}}(n+1) &= \tilde{\boldsymbol{A}}\tilde{\boldsymbol{x}}(n), \\ s(n) &= \tilde{\boldsymbol{C}}\boldsymbol{x}(n) + \mathrm{E}(n), \end{aligned} \tag{15}$$

where $\tilde{\boldsymbol{A}} = \boldsymbol{P}\boldsymbol{A}\boldsymbol{P}^{-1}$ and $\tilde{\boldsymbol{C}} = \boldsymbol{C}\boldsymbol{P}^{-1}$ are real-valued matrices and $\tilde{\boldsymbol{x}} = [\boldsymbol{r}_0\ \mathrm{Re}(\boldsymbol{r}_1)\ j\mathrm{Im}(\boldsymbol{r}_1)\ \dots\ \mathrm{Re}(\boldsymbol{r}_h)\ j\mathrm{Im}(\boldsymbol{r}_h)]$.

Application of the Kalman Filter and Coefficient Estimation

The standard discrete Kalman filter[24][25] can be applied to obtain the estimate of the harmonic components using the model (Equation 12). The Kalman filter implementation is shown in Algorithm 1. After the filtering process. The amplitudes and phases of each component $c_h(t)$, as well as its derivatives, can be derived from the estimates of $\tilde{\boldsymbol{x}}$.

ALGORITHM 1. **Pseudocode of the Kalman Filter**

---

procedure
Initialize parameters.
for each sample n
Predict state:

$$\tilde{\boldsymbol{x}}^{-}(n) = \tilde{\boldsymbol{A}}\tilde{\boldsymbol{x}}^{-}(n-1)$$

Predict covariance:

$$\boldsymbol{P}^{-}(n) = \tilde{\boldsymbol{A}}\boldsymbol{P}(n-1)\boldsymbol{A}'$$

Update Kalman gain:

$$\boldsymbol{K}(n) = \boldsymbol{P}^{-}(n)\tilde{\boldsymbol{C}}'(\tilde{\boldsymbol{C}}\boldsymbol{P}^{-}(n)\tilde{\boldsymbol{C}}' + \sigma_e^2)^{-1}$$

Update state.

$$\tilde{\boldsymbol{x}}(n) = \tilde{\boldsymbol{x}}^{-}(n) + \boldsymbol{K}(n)\left(s(n) - \tilde{\boldsymbol{C}}\tilde{\boldsymbol{x}}^{-}(n)\right)$$

Update covariance.

$$\boldsymbol{P}(n) = (\boldsymbol{I} - \boldsymbol{K}(n))\tilde{\boldsymbol{C}}\boldsymbol{P}^{-}(n)$$

end for
end procedure

RESULTS AND DISCUSSION

In this section, the estimates of the TKA filter are illustrated and compared with the Sgolay, NTD, ESO, and DDTS methods. The test signals are ECG, RAW (data corresponding to heart R-wave to R-wave

intervals), and blood pressure. As the first test signal, a synthetic ECG is developed with mathematical functions to obtain its derivative, using the set of derivatives of each of its functions. Hence, the estimation error in the signal and its derivative can be obtained. However, since the derivative in the measurement signals is not known, the error is only calculated with respect to the measurement signal.

Performance Results of the TKA Filter

The performance of the algorithm is showcased in this section, utilizing a polynomial approximation of $K = 2$ and $H = 64$ harmonics as detailed in Equation 4. In what follow we evaluate the capacity to reconstruct the input signal after applying the analysis and synthesis stages for the proposed real-valued TKA (Taylor-Kalman Algorithm). For the TKA, the analysis stage includes the state estimation using the Kalman algorithm, and then the synthesis stage computes a reconstruction of the input signal from the filter estimates. We also evaluate the performance of the TKA as a derivative are also computed. The proposed TKA Filter was implemented on a computer with Matlab 2016b, Intel Core i5 @ 2.6 GHz, 8.00 GB RAM, and operative system Mojave for MacOS is used.

As the PhysioNet signals[26] have not information about the derivative of the measurement signal. There is a problem when the performance of the derivative estimation is evaluated. To solve this situation, a math model of ECG is used to create synthetic ECG signals with known derivatives, obtained with each function of (Equation 16). The used model was proposed in[27], the synthetic ECG signal is defined as follows (Equation 16):

$$f_0(t) = 0, \qquad 0 \le t \le 200 \tag{16.a}$$

$$f_1(t) = a - \frac{\frac{a}{100}}{15}\left(\frac{8}{b}\left(t - \left(200 + \frac{b}{2}\right)\right)\right)^2, \qquad 200 \le t \le 200 + b \tag{16.b}$$

$$f_2(t) = 0, \qquad 200 + b \le t \le 440 \tag{16.c}$$

$$f_3(t) = \left[\frac{140-d}{100}\, g + 1\right] c\left[\frac{-1.1*0.3(t-440)}{20}\right], \qquad 440 \le t \le 440 + \frac{d}{7} \tag{16.d}$$

$$f_4(t) = \left[\frac{140-d}{100}\, g + 1\right] c\left[\frac{-1.1*0.6(t-[400+1.5\frac{d}{7}])}{20}\right], \qquad 440 + \frac{d}{7} \le t \le 440 + 3\frac{d}{7} \tag{16.e}$$

$$f_5(t) = \left[\frac{140-d}{100}\, g + 1\right] c\left[\frac{-1.1*0.5(t-[400+5\frac{d}{7}])}{20}\right], \qquad 440 + 3\frac{d}{7} \le t \le 440 + 6\frac{d}{7} \tag{16.f}$$

$$f_6(t) = \left[\frac{140-d}{100}\, g + 1\right] c\left[\frac{-1.1*0.5(t+440)}{20}\right], \qquad 440 + 6\frac{d}{7} \le t \le 440 + d \tag{16.g}$$

$$f_7(t) = 0, \qquad 440 + d \le t \le 440 + d + 680 \tag{16.h}$$

$$f_8(t) = a - \frac{\frac{e}{100}}{15}\left(\frac{80}{f}\left(t - \left(680 + \frac{f}{2}\right)\right)\right)^2, \qquad 440 + d \le t \le 440 + d + f. \tag{16.i}$$

The range for each one of the variables $a \cdots g$ used in the definition of the synthetic ECG is show in the Table 1.

TABLE 1. Parameters of the synthetic ECG signal.

Variable	Function in synthetic ECG signal	Physiological interval
a	Amplitude of P wave	0-0.3 mV
b	Length of P wave	0-160 ms
c	Amplitude of the QRS complex	0-0.5 mV
d	Length or QRS complex	50-120 ms
e	Amplitude of T wave	0-0.8 mV
f	Length of T wave	0-300 ms
g	Amplitude of the QRS complex	0-50 mV

In Figure 1. The signal estimates are illustrated in top of the graph, while the derivative estimates are illustrated in bottom of the graph, the parameters used to generate the synthetic signal for this example are a = 0.1, b = 160, c = 0.096, d = 120, e = 0.2, f= 300, g = 50.

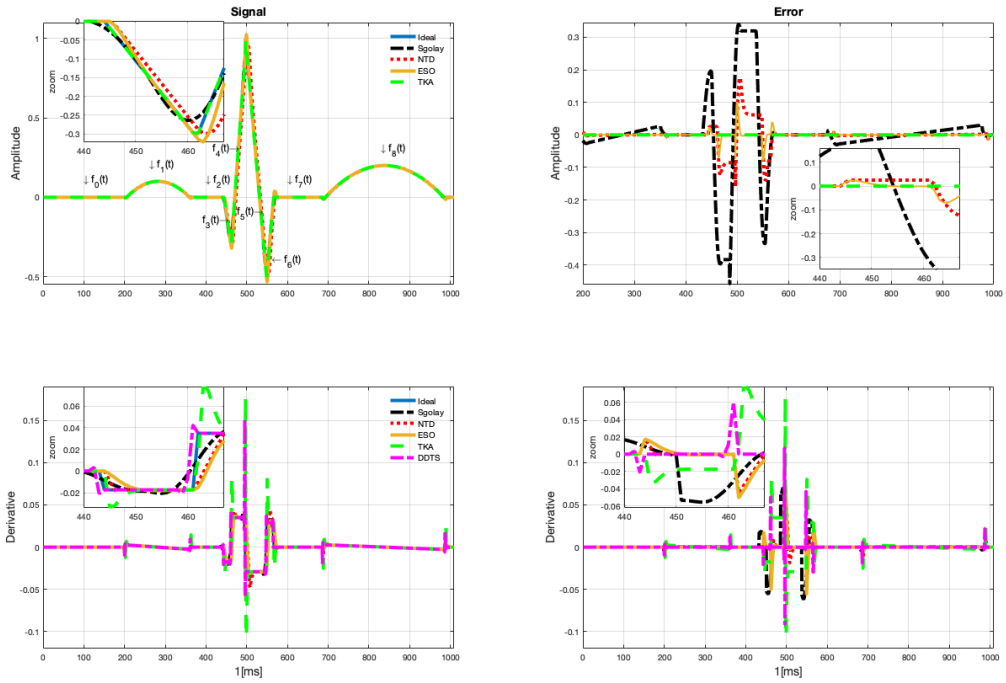

FIGURE 1. Synthetic ECG signal and derivative estimates with Sgolay, NTD, ESO, DDTS, and TKA.

The input signal, as well as the estimates from the four algorithms, are displayed in Figure 1, (the measurement is illustrated in left top graph, and the error estimate in the right top graph). Furthermore, a zoomed-in view is offered to facilitate a closer examination of the estimation details. As it can be seen, the Sgolay estimation smooths (filters out high-frequency signals), which can lead to estimation errors in some cases or segments of the signal. On the other hand, NTD estimation provides errors in sections with abrupt changes in amplitude. And the ESO estimates have a similar behavior to the NTD but with greater amplitude. It can be observed that signal estimates provided by the proposed TKA method have the best performance. In

Figure 1, left of bottom graph, the estimation of the derivative of the signal is shown, which corresponds to the same zoomed-in section of the signal. Similarly, in the derivative estimation, the Sgolay method tends to smooth the signal, NTD method provides a significant number of errors when the signal exhibits rapid changes in amplitude. It is important to remark that no additional differentiator algorithms are needed to compute the estimation of the derivative when the proposed Kalman algorithm is used. Also, the error in derivative estimation is shown in the bottom right graph in Figure 1. When an abrupt change in the signal occurs, the estimations have considerable errors, with better estimates obtained using the ESO and DDTS methods. However, the measurement signals are smoother than the synthetic signal.

Signal under estimation is an Electrocardiogram (ECG) signal sourced from the PhysioNet database[26], (Signals recorded in labor, between 38 and 41 weeks of gestation; four signals acquired from maternal abdomen; direct electrocardiogram recorded simultaneously from fetal head; positioning of electrodes was constant during all recordings; Ag-AgCl electrodes (3M Red Dot 2271) and abrasive material to improve skin conductance (3M Red Dot Trace Prep 2236); bandwidth: 1Hz - 150Hz (synchronous sampling of all signals); additional digital filtering for removal of power-line interference (50Hz) and baseline drift, Sampling rate: 1 kHz; resolution: 16 bits; input ranges are included in the records in EDF format). On the other hand, the results are depicted in Figure 2, where the estimation is compared with the Sgolay, NTD, ESO and TKA, The DDTS cannot estimate the signal; it can only estimate the derivative of the signal. As can be seen in the zoomed area, better estimates of the signal are obtained with TKA. The Sgolay filter smooths the changes, while NTD and ESO provide similar estimates. However, the ESO method yields larger estimates in amplitude. The derivative estimate is shown in the graph in Figure 2. Unlike the synthetic signal, DDTS provided the worst case in the estimates and is illustrated in yellow to distinguish it from the other signal estimates. The derivative estimates with TKA improve, with regard to the synthetic signal due to the smooth changes in the amplitude of the derivative.

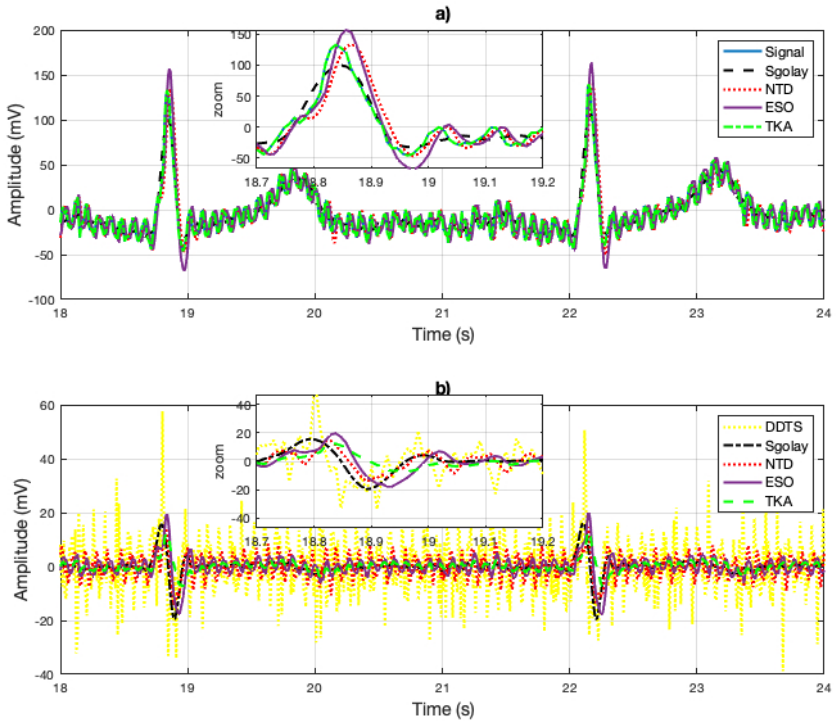

FIGURE 2. **a) Signal reconstruction with the Sgolay, NTD, ESO and TKA methods. And Zoomed-in view of the reconstructed (estimated) signal. In b) the derivative estimates are illustrated and zoomed-in view of the derivative estimation of the signal.**

As a third example, a cardiorespiratory signal RAW (data corresponding to heart R-wave to R-wave intervals). Data correspond to heart R-wave to R-wave intervals, Oxygen consumption, and mechanical power output on a beat-to-beat basis recorded all along the graded exercise test sessions. Participants are 18 teenagers athletes (15.2±2 years) from the Regional Physical and Sports Education Centre (CREPS) of French West Indies (Guadeloupe, France)[26]. The results obtained using the Sgolay, NTD, ESO and TKA methods illustrated in Figure 3.a). In figure, a zoomed-in view of the signal is shown. Similarly to Figure 2, the estimates for rapid changes in the signal are deficient with the Sgolay and NTD methods. The DDTS method produced large errors when the signal had abrupt changes. In Figure 2 b), a close-up of the derivative estimation is presented, and the results show a behavior very similar to the derivative signal estimates in the electrocardiogram.

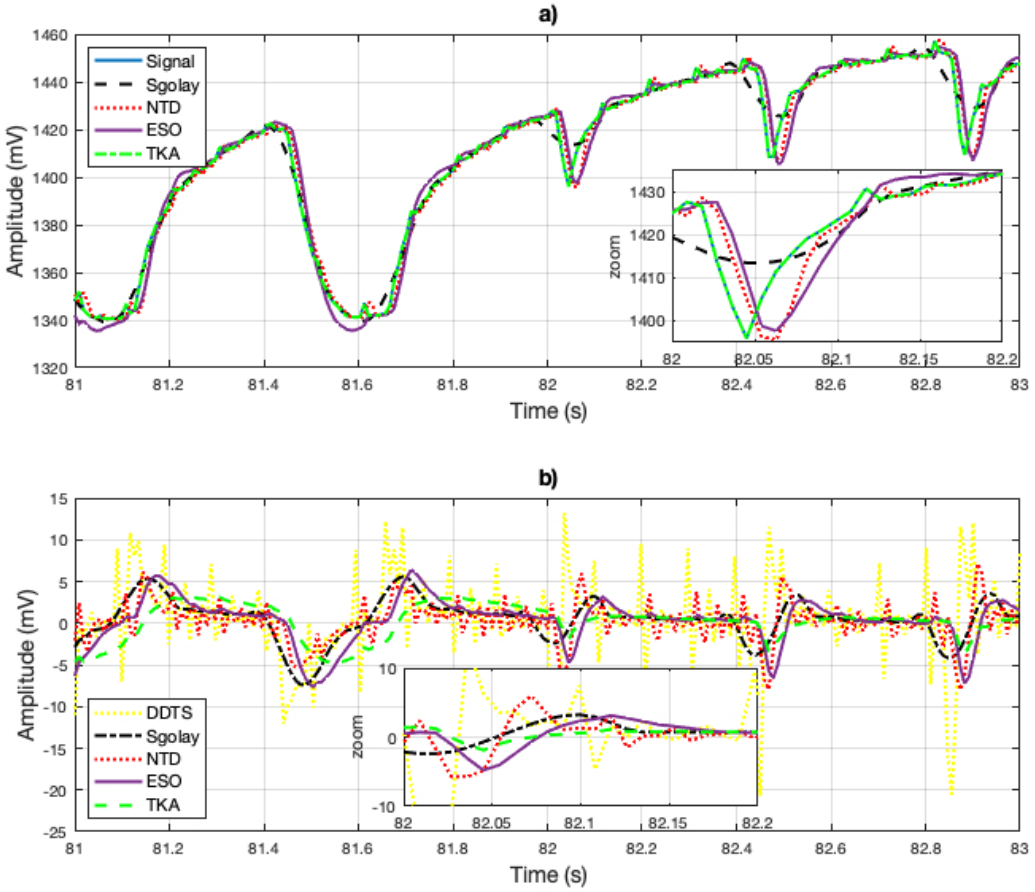

FIGURE 3. a) Signal reconstruction using the Sgolay, NTD, ESO and TKA methods. b) Zoomed-in view of the estimation. c) Estimation of the derivative of the estimated signal and include the derivative estimation with DDTS.

In Table 2, the RMSE error (17) estimates in signal and derivative estimate are show, as can be seen, TKA provided the better signal reconstruction. The best derivative estimates of the synthetic signal were obtained by NTD, the estimates in TKA are degraded by the transients, however they are closer to the NTD estimates and can be obtained without an additional derivative stage. The derivative of the synthetic signal is provided by the derivative of each function $(f_0(t), f_1(t), \ldots, f_8(t))$. However, since the measurement signal does not provide a known derivative, the error is not calculated. To obtain the derivative of the measurement signal, it would need to be processed by another method. Hence, in Table 2, only the error of the signal is calculated.

TABLE 2. RMSE in signal and derivative estimates.

Signal		RMSE				
		METHOD				
		Sgolay	NTD	ESO	DDTS	TKA
Synthetic	Signal	0.0059	0.0311	0.0102	Not applicable	7.2722×10^{-5}
	Derivative	0.1821	0.006	0.0059	0.0061	0.0089
ECG	Signal	12.0219	12.9263	13.7664	Not applicable	7.7915×10^{-5}
RAW	Signal	4.4964	5.6750	7.4522	Not applicable	1.1348×10^{-5}
Blood	Signal	1.5211×10^{-4}	0.2916	0.0577	Not applicable	4.1782×10^{-15}
RAW 2	Signal	0.0475	0.0525	0.0656	Not applicable	1.4625×10^{-15}

As a reference for the accuracy of the estimations, the root mean square error (RMSE) is calculated, which is defined as (Equation 17):

$$\text{RMSE} = \sqrt{\frac{\sum(s(n) - \hat{s}(t))^2}{N}} \tag{17}$$

where $s(n)$ represents the input signal and the signal estimation is defined as $\hat{s}(t)$ and N is the ample size.

CONCLUSIONS

The objective of this work is to verify the efficiency of TKA for the estimation of biomedical signals; three types of biomedical signals (ECG, synthetic ECG, cardiorespiratory and blood pressure) were analyzed. The capacity for signal reconstruction and derivative estimation were compared with the Sgolay, NTD, ESO and DDTS methods. Also, the estimation of the input signal is not obtained by the DDTS method, because it can only estimate the derivative of the signal. The results obtained for signal estimation show an advantage over the Sgolay, NTD and ESO methods, as well as a superiority in the estimation of its first derivative compared to the ESO method. On the other hand, note that the estimation is with respect to the synthetic derivative of the ECG signal, which has large discontinuities. Hence, in measurement signals that are smoother, it could be expected that the estimates in the derivative would have more precision. Looking ahead, to enhance the generalizability of our findings, we plan to extend our testing to include a wider array of real physiological signals like EMG and EEG.

ACKNOWLEDGEMENT

All the authors acknowledge the research grant CF-2023-I-1110 from CONAHCYT (Mexico) and the support from the "Departamento de Electrónica y Automatización" at the Facultad de Ingeniería Mecánica y Eléctrica, UANL.

All the authors acknowledge to PhysioNet,[15] a public collection of biomedical signals.

AUTHOR CONTRIBUTIONS

J. R. M. data curation, investigation, methodology, project administration, software, visualization, and writing original draft; E. Z. S. conceptualization, formal analysis, funding acquisition, and resources; M. A. P. G. supervision, validation, and writing review and editing.

REFERENCES

[1] W. Bouaziz, E. Schmitt, G. Kaltenbach, B. Geny and T. Vogel, "Health benefits of cycle ergometer training for older adults over 70: a review," Eur. Rev. Aging. Phys. Act., vol. 12, Nov. 2015, Art. no. 8, doi: https://doi.org/10.1186/s11556-015-0152-9

[2] R. M. Rangayyan, Biomedical Signal Analysis, 2nd ed. Wiley-IEEE Press, 2015.

[3] K. Najarian and R. Splinter, Biomedical Signal and Image Processing, 2nd ed. Boca Raton, FL, United State: CRC Press, 2012, doi: https://doi.org/10.1201/b11978

[4] R. M Rangayyan, Biomedical Signal Analysis: A Case-Study Approach, Wiley-IEEE Press, 2002.

[5] T. U. Zaman, D. Hossain, T. Arefin, A. Rahman, S. N. Islam, F. Haque, "Comparative analysis of de-noising on ECG signal," Int. J. Emerging Technol. Adv. Eng., vol. 2, no. 11, pp. 479-486, 2012.

[6] N. Pombo, B. M. C. Silva, A. M. Pinho, and N. Garcia, "Classifier Precision Analysis for Sleep Apnea Detection Using ECG Signals," IEEE Access, vol. 8, pp. 200477-200485, 2020, doi: https://doi.org/10.1109/ACCESS.2020.3036024

[7] L. R. Castro and S. M. Castro, "Wavelets y sus aplicaciones," in I Congreso Argentino de Ciencias de la Computación, Argentgina, Oct. 1995. [Online]. Available: http://sedici.unlp.edu.ar/handle/10915/24289

[8] G. Saripalli, P. H. Prajapati, and A. D. Darji, "CSD Optimized DWT Filter for ECG Denoising," in 2020 24th International Symposium on VLSI Design and Test (VDAT), Bhubaneswar, India, 2020, pp. 1-6, doi: https://doi.org/10.1109/VDAT50263.2020.9190624

[9] J. Feng, G. Li, W. Wang, and X. Liang, "The Application of Improved Tracking-differentiator Filter in ECG Data," DEStech, Apr. 2018, doi: https://doi.org/10.12783/dtcse/mso2018/20519

[10] Y. Tang, Y. Wu, M. Wu, X. Hu, and L. Shen, "Nonlinear Tracking-Differentiator for Velocity Determination Using Carrier Phase Measurements," IEEE J. Sel. Top. Signal Process., vol. 3, no. 4, pp. 716-725, Aug. 2009, doi: https://doi.org/10.1109/JSTSP.2009.2024591

[11] J. Rodríguez-Maldonado, C. Posadas-Castillo, and E. Zambrano-Serrano, "Alternative Method to Estimate the Fourier Expansions and Its Rate of Change," Mathematics, vol. 10, no. 20, Jan. 2022, Art. no. 20, doi: https://doi.org/10.3390/math10203832

[12] J. Rodriguez Maldonado, "Total Harmonic Distortion Estimation, Minimization Inter Harmonic Amplitude and Expanding Bands Rejection in TKF filters," IEEE Lat. Am. Trans., vol. 14, no. 2, pp. 652-656, Feb. 2016, doi: https://doi.org/10.1109/TLA.2016.7437206

[13] J. Han, "A Class of Extended State Observers for Uncertain Systems," Control Dec., vol. 10, no. 1, pp. 85-88, 1995.

[14] B.-Z. Guo, Z.-L. Zhao, "Extended state observer for nonlinear systems with uncertainty," IFAC Proc. Vol., vol. 44, no. 1, pp. 1855-1860, 2011, doi: https://doi.org/10.3182/20110828-6-IT-1002.00399

[15] J. L. Vargas-Luna, W. Mayr, and J. A. Cortés-Ramírez, "Amplitude Modulation Approach for Real-Time Algorithms of ECG-Derived Respiration," Rev. Mex. Ing. Biomed., vol. 35, no. 1, pp. 53-69, 2014.

[16] J. R. Cárdenas-Valdez, F. Ramírez-Arzate, Á. H. Corral-Domínguez, C. Hurtado-Sánchez, A. Calvillo-Téllez, and E. E. García-Guerrero, "Development of an Adaptive Acquisition and Transmission System for Digital Processing of ECG Signals under Variable n-QAM Schemes," Rev. Mex. Ing. Biomed., vol. 44, no. 4, pp. 117-127, 2023, doi: https://doi.org/10.17488/RMIB.44.4.8

[17] M. E. Cano, R. A. Jaso, M. E. Tavares, J. C. Estrada, et al., "A simple alternative for modulating and recording the PQRST complex," Rev. Mex. Ing. Biomed., vol. 32, no. 2, pp. 100-108, Dec. 2011.

[18] D. Torres Guzmán and C. S. Carbajal Fernández, "Mejora de la Señal de Flujo Sanguíneo en Implantes Coronarios Mediante la Detección de Distorsiones Eventuales," Rev. Mex. Ing. Biomed., vol. 36, no. 1, pp. 33-53, 2015.

[19] X. Ning and I. W. Selesnick, "ECG Enhancement and QRS Detection Based on Sparse Derivatives," Biomed. Signal Process. Control, vol. 8, no. 6, pp. 713-723, Nov. 2013, doi: https://doi.org/10.1016/j.bspc.2013.06.005

[20] C. Lastre-Domínguez, O. Ibarra-Manzano, J. A. Andrade-Lucio, and Y. S. Shmaliy, "Denoising ECG Signals Using Unbiased FIR Smoother and Harmonic State-Space Model," 2020 28th European Signal Processing Conference (EUSIPCO), Amsterdam, Netherlands, 2021, pp. 1279-1283, doi: https://doi.org/10.23919/Eusipco47968.2020.9287522

[21] I.R. Khan, R. Ohba, "New design of full band differentiators based on taylor series," IEE Proc. - Vis. Image Signal Process., vol. 146, no. 4, pp. 185-189, 1999, doi: https://doi.org/10.1049/ip-vis:19990380

[22] P. H. Langner and D. B. Geselowitz, "First Derivative of the Electrocardiogram," Circ. Res., vol. 10, pp. 220-226, Feb. 1962, doi: https://doi.org/10.1161/01.res.10.2.220

[23] J. Rodriguez Maldonado and M. A. Platas Garza, "Comparative Load Reduction and Analysis of Taylor Kalman Fourier Filters in Synchrophasor Measurement," IEEE Lat. Am. Trans., vol. 16, no. 8, pp. 2153-2160, Aug. 2018, doi: https://doi.org/10.1109/TLA.2018.8528229

[24] D. G. Manolakis, V. K. Ingle, and S. M. Kogon, Statistical and Adaptive Signal Processing: Spectral Estimation, Signal Modeling, Adaptive Filtering and Array Processing. Boston, United State: Artech House Publishers, 2005.

[25] D. Simon, Optimal State Estimation: Kalman, H Infinity, and Nonlinear Approaches. Hoboken, JN, United State: John Wiley & Sons, 2006, doi: https://doi.org/10.1002/0470045345

[26] C. Chabert, D. Mongin, E. Hermand, A. Collado, and O. Hue, "Cardiorespiratory measurement from graded cycloergometer exercise testing (version 1.0.0)", PhysioNet, doi: https://doi.org/10.13026/2qs3-kh43

[27] J. Kubicek, M. Penhaker, and R. Kahankova, "Design of a synthetic ECG signal based on the Fourier series," 2014 International Conference on Advances in Computing, Communications and Informatics (ICACCI), Delhi, India, 2014, pp. 1881-1885, doi: https://doi.org/10.1109/ICACCI.2014.6968312